

# One Sparse Perturbation to Fool them All, almost Always!

Arka Ghosh<sup>1</sup>, Sankha Subhra Mullick<sup>2</sup>, Shounak Dutta<sup>3</sup>, Swagatam Das<sup>4</sup>, Rammohan Mallipeddi<sup>5</sup>, and Asit Kr. Das<sup>6</sup>

<sup>1,6</sup>Dept. of Computer Sc. & Tech. IIST Shibpur

<sup>2</sup>Electronics and Communication Sciences Unit, Indian Statistical Institute, Kolkata, India

<sup>3</sup>Electrical and Computer Engineering Dept., Duke University, USA

<sup>4</sup>Electronics and Communication Sciences Unit, Indian Statistical Institute, Kolkata, India

<sup>5</sup>Department of Artificial Intelligence, School of Electronics Engineering, Kyungpook National University, Daegu, 41566, Republic of Korea

April 2020

## Abstract

Constructing adversarial perturbations for deep neural networks is an important direction of research. Crafting image-dependent adversarial perturbations using white-box feedback has hitherto been the norm for such adversarial attacks. However, black-box attacks are much more practical for real-world applications. Universal perturbations applicable across multiple images are gaining popularity due to their innate generalizability. There have also been efforts to restrict the perturbations to a few pixels in the image. This helps to retain visual similarity with the original images making such attacks hard to detect. This paper marks an important step which combines all these directions of research. We propose the DEceit algorithm for constructing effective universal pixel-restricted perturbations using only black-box feedback from the target network. We conduct empirical investigations using the ImageNet validation set on the state-of-the-art deep neural classifiers by varying the number of pixels to be perturbed from a meagre 10 pixels to as high as

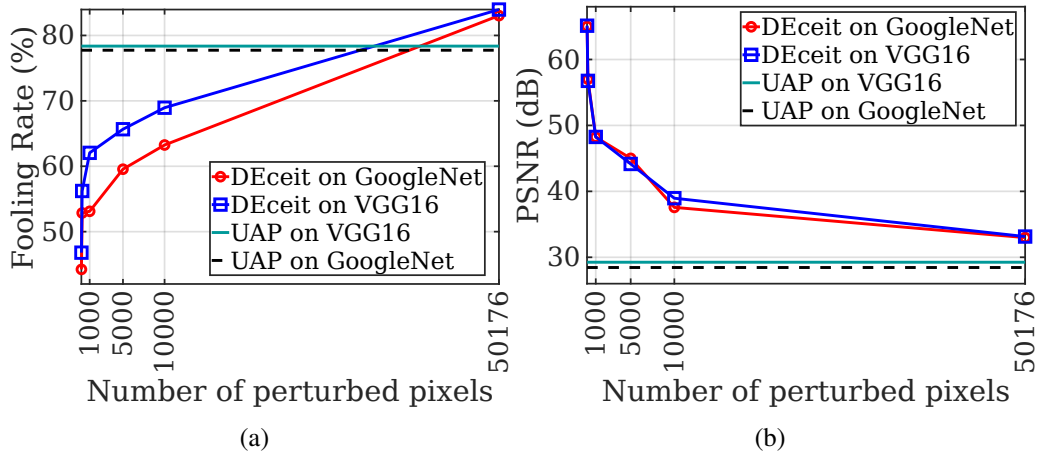


**Figure 1:** We compare the quality of universal adversarial perturbations generated by DEceit with increasing number of perturbed pixels (respectively 10, 100, 1000, 5000, 10000, and all of 50176 pixels in images of resolution  $224 \times 224$ ) on the ImageNet validation set, for two state-of-the-art deep neural network classifiers, viz. VGG16 and GoogleNet. To compensate for the extremely low number of pixels, the allowable distortion is set to  $[-128, 128]$  for 10 pixels,  $[-30, 30]$  for 100 pixels,  $[-20, 20]$  for 1000 pixels and the conventional  $[-10, 10]$  thereafter. (a) When all pixels are allowed to be perturbed, DEceit (our proposed black-box method) achieves a better Fooling Rate (FR) than the white-box UAP [15] on both classifiers. Moreover, DEceit achieves a commendable FR of 66% and 60% respectively on VGG16 and GoogleNet when only 5000 pixels are allowed to be perturbed. This indicates that it is indeed feasible to generate an effective universal perturbations by only modifying a restricted number of pixels. (b) DEceit also achieves better PSNR values compared to UAP indicating a higher similarity of the perturbed image with the corresponding original.

all pixels in the image. We find that perturbing only about 10% of the pixels in an image using DEceit achieves a commendable and highly transferable Fooling Rate while retaining the visual quality. We further demonstrate that DEceit can be successfully applied to image dependent attacks as well. In both sets of experiments, we outperformed several state-of-the-art methods.

## 1 Introduction

The Convolutional Neural Networks (CNN) are susceptible to perturbations in the input [28] even after demonstrating remarkable efficiency on challenging computer vision tasks, akin to the vulnerable heel of the mighty Achilles. As CNNs are being increasingly deployed in critical applications like autonomous driving, fraud detection, etc. their sensitivity to perturbations can result in serious adversity. This inspired the research community to consider the study of adversarial perturbations as immensely important and subsequently venture diverse schools of thought.

Adversarial perturbations can be devised using two main strategies, viz. white-box and black-box attacks. In the white-box setting, which has been widely explored [2, 8, 16], the attacker has full access to the parameters, the gradients of the loss function concerning the target class label(s) to the input image(s), and the

architecture of the CNN which is to be attacked. In contrast, in the relatively less explored black-box setting [21], the attacker only has access to the decisions made by the target classifier. Since black-box approaches like [4, 9] do not rely on any classifier-intrinsic information, the resulting perturbations generally have greater transferability compared to white-box attacks. Moreover, black-box attacks are more practical as model-specific information is often unavailable in real-world settings.

From a different perspective, adversarial attacks on CNNs can also be classified into image-dependent and universal categories. Image-Dependent Attacks (IDA) like [14, 30] allow distinct perturbations to be employed for different images, resulting in a significant loss of the classification accuracy for the target CNN. Universal Adversarial Attacks (UAAs) like [15, 17, 18, 22], on the other hand, attempt to craft perturbations which can be applied to any natural image (irrespective of content and provenance) to mislead the target classifier. As a result, UAAs generally exhibit better generalizability to previously unseen images. Moreover, UAAs are also more computationally efficient as there is no need to recompute perturbations for every individual image.

Another emerging direction of research [19] investigates the potential for misleading the CNN classifiers by perturbing a limited number of pixels in the images. The authors in [26] attempted to test the extent of such restricted image dependent perturbation and found that manipulating merely a single pixel can result in a successful attack. This suggests that identifying and perturbing the pixels which are most critical for classification (as opposed to perturbing the entire image) may be sufficient to induce misclassification. Further, limiting the number of pixels to be perturbed generally results in perturbations which are imperceptible to human eyes. Such attacks are especially menacing as they can pass undetected even if the autonomous system is accompanied by human users.

In light of the above discussion, in this article, we attempt for the first time, to devise pixel-restricted i.e. sparse perturbations for universal attacks by using black-box feedback. The pixel-restriction means that we must identify the most critical pixels among a potentially large number of pixels, depending on the size of the input images. Moreover, the optimization problem by nature is extremely high-dimensional (for example, given a RGB image of resolution  $224 \times 224$ , in case of DEceit the dimension of the problem may reach a maximum of 250880 when all pixels are allowed to be perturbed). Consequently, a brute-force search of the whole search space is not computationally feasible. Moreover, the black-box setting means that no gradient information is available from the target CNN, ruling-out the use of gradient-based optimization schemes. To address this issue, we propose to use a powerful population-based stochastic optimization technique called Differential Evolution (DE) [25] to find suitable perturbations. DE is remarkably efficient over diverse optimization scenarios like constrained, multi-

modal, multi-objective problems, owing to the decades of research effort devoted to improving its scalability, convergence [20], and robustness [5]. Recently, SwitchDE [7] showed that a simple parameter, as well as mutation switching strategy, can be very effective for high-dimensional optimization problems by achieving an effective trade-off between the exploratory and exploitative search behaviors of DE. Our proposed DE based adversarial perturbation generation scheme, DEceit, combines the mutation switching strategy from SwitchDE with uniform random scale-factor switching (see Section 3.4) to effectively solve the high-dimensional optimization problem. The effectiveness of DEceit in comparison to UAP is illustrated in Figure 1, which validates that even by perturbing merely 10% of total number of pixels DEceit can achieve an admirable Fooling Rate (FR) on both CNNs while maintaining a better visual quality.

The principal highlights of our proposal are in order:

1. We add to the existing literature by proposing DEceit, which is capable of crafting effective universal perturbations by modifying only a small fraction of the fixed pixels for any image using just black-box feedback from the network under attack. This combines the practicality of the black-box setting with the robustness of UAAs while keeping the perturbed images similar to the original images, making detection and prevention challenging.
2. Unlike [1, 26] we consider the large scale and high-dimensional nature of the optimization problem related to adversarial perturbations. Hence, we have synthesized the DEceit algorithm by augmenting the DE with two fundamental changes: a random parameter switching strategy and the success-based mutation strategy adopted from [7]. Further, we employ a simple encoding scheme which can inherently impose the sparsity constraint.
3. We demonstrate that DEceit can directly be used to construct effective image-dependent perturbations as well.

Subsequent to the introductory Section 1, we establish the background in Section 2 and detail DEceit in Section 3. In Section 4 we carry out an extensive comparison with the state-of-the-art techniques to establish the capability of DEceit to generate sparse perturbations which can effectively perform UAA and IDA in a black box setting. Finally, we make concluding remarks and discuss future extensions in Section 5.

## 2 Related Works

The work of [19] has recently been carried forward by researches such as [3, 13, 26] which showed that sparse perturbations are not only effective but are also likely to

offer better imperceptibility. However, these notable attempts for generating sparse and efficient adversarial perturbation have only been applied for IDAs. In case of UAAs the complexity of the problem considerably increases as it becomes even more difficult to find a limited set of pixels, modifying which will affect a large set of images containing variety of objects in differing scales, lighting conditions, etc.

Evolutionary Optimization (EvO) algorithms gained popularity in devising adversarial perturbations as they can handle large scale problems and are especially useful in black box setting. A couple of works [1, 26] attempted to respectively utilize DE and Genetic Algorithm (GA) to carry out successful IDA. However, as discussed earlier, the underlying optimization problem is extremely high dimensional in nature which [1] did not consider and [26] avoided by restricting themselves to one pixel attack. This led them to rely on the canonical variants of the EvO algorithms which alongside being ineffective in large scale optimization problem are susceptible to the curse of dimensionality.

### 3 Proposed Method

An image  $I$  is conventionally represented in the form of a third-order tensor i.e.  $I \in \mathbb{R}^{w \times h \times c}$ , where  $w$ ,  $h$  and  $c$  are positive integers respectively denoting the width, height and the number of channels of the image. Depending on the application, the components of  $I$  can be further constrained and bounded. Here, for simplicity without loss of generality, we assume any component  $I_{pqr} \in [0, 255]$ , for all  $p \in [1, w]$ ,  $q \in [1, h]$ , and  $r \in [1, c]$ , where  $[a, b]$  denotes the closed set of all integers between  $a$  and  $b$ . Further, let a dataset  $\mathcal{S} = \{I_1, I_2, \dots, I_m\}$  be a collection of  $m$  images, where each image can be classified into one of the  $C$  predefined classes. Classification can be represented as finding the many-to-one mapping  $y : \mathcal{S} \rightarrow \mathcal{C}$ , where  $\mathcal{C} = \{1, 2, \dots, C\}$ . CNN classifiers, being supervised learning algorithms, attempt to approximate  $y$  as  $\hat{y}$ , utilizing the information provided through a set  $\mathcal{X} \subseteq \mathcal{S}$  of training examples such that for all  $I \in \mathcal{X}$  the true class label  $y(I)$  is known in advance.

#### 3.1 Universal Attack

The vulnerability of CNNs to adversarial attack may originate from its learning mechanism. The decision strategy learned by the network to correctly identify a class can be effectively exploited by a perturbation leading to a misclassification [12]. This indicates the possibility of a UAA attack exploiting an amalgamation of the network’s decision strategies for the individual classes.

Given an original image  $I \in \mathcal{S}$  which is correctly classified as belonging to the class,  $j \in \mathcal{C}$ , a perturbed image is created as  $\bar{I} = \psi(I + \Delta)$ , where  $\Delta \in \mathbb{R}^{w \times h \times c}$

is a perturbation tensor and  $\psi(\cdot)$  is a function ensuring (by proper scaling and/or bounding) that the addition adheres to the properties of an image. Hence, our objective of designing a UAA can be reduced to finding a perturbation  $\Delta$ , which maximizes the probability of misclassifying  $\bar{I}$ :

$$\max \mathcal{P}(\Delta) = \sum_{I \in \mathcal{S}} Pr(\hat{y}(\psi(I + \Delta)) \neq j), \quad (1)$$

$$\text{s.t. } -\beta \leq \Delta_{pqr} \leq \beta, \quad (2)$$

where  $\beta$  is an user-defined parameter controlling the extent of distortion in one component of the perturbation tensor  $\Delta_{pqr}$  for all  $p \in [1, w]$ ,  $q \in [1, h]$ ,  $r \in [1, c]$ , and  $Pr(\cdot)$  denotes the probability of an event.

### 3.2 Sparse Perturbation

Perturbing every pixel of an image may lead to a compromised visual quality. An attractive alternative may come in the form of sufficient perturbation of limited number of critical pixels. Such a perturbation will likely be capable of performing a successful attack alongside improved imperceptibility. This would enable the UAA to be sparse in nature, consequently improving the visual similarity between the original images and the corresponding perturbed images. However, such a sparsity constraint poses additional difficulty for the high-dimensional UAA search problem. First, one needs to recognize the pixels which are critical for correctly identifying a majority of the classes. Thereafter, a suitable subset containing a predetermined number of pixels must be selected and efficiently perturbed to obtain the optimal sparse universal perturbation.

### 3.3 Black-Box Feedback

The challenge of finding an effective adversarial perturbation further increases in a black-box setting, which restricts utilization of the image-to-class decision mappings expressed through the network architecture and learned parameters. However, such restrictions allow a black-box method to be independent of the CNN under attack. Consequently, perturbation obtained through black-box methods is expected to provide improved robustness and transferability compared to those found by white-box attacks. For a black-box setting, one may choose to maximize the FR i.e. the number of misclassified images, instead of directly maximizing the probability of misclassification. Thus, the optimization problem in (1) can be

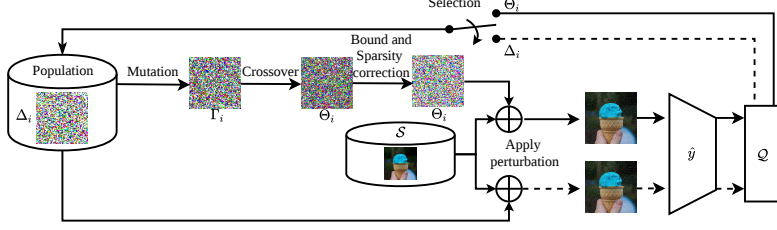


**Figure 2:** DEceit attempts to iteratively improve the quality of a population of candidate perturbations (number of pixel to be perturbed  $\rho = 5000$  and distortion  $\beta = 10$ ) to find the optimal solution of  $\mathcal{Q}$ . First a parent perturbation  $\Delta_i$  for all  $i = 1, 2, \dots, n$  is mutated to generate  $\Gamma_i$ . Subsequently,  $\Gamma_i$  and  $\Delta_i$  go through a crossover step to form  $\Theta_i$ . The perturbation  $\Theta_i$  may not adhere to the constraints of  $\mathcal{Q}$ , and thus the bound restriction is imposed. Finally,  $\mathcal{Q}(\Delta_i)$  and  $\mathcal{Q}(\Theta_i)$  are both applied to the set  $\mathcal{S}$  of images and evaluated.  $\Theta_i$  replaces  $\Delta_i$  in the population if found to better optimize  $\mathcal{Q}$ , i.e.  $\mathcal{Q}(\Delta_i) \geq \mathcal{Q}(\Theta_i)$ . Note that the perturbations are color inverted for the ease of visualization while their encoding/decoding which might be necessary for the implementation of DEceit are ignored for simplicity.

revised for a sparse black-box setting as follows:

$$\max \mathcal{Q}(\Delta) = \sum_{I \in \mathcal{S}} \mathcal{I}(\hat{y}(\psi(I + \Delta)) \neq y(I)), \quad (3)$$

$$\text{s.t. } -\beta \leq \Delta_{pqr} \leq \beta, \quad (4)$$

$$\text{and } \sum_{p=1}^w \sum_{q=1}^h \mathcal{I}(\Delta_{pq} \neq 0) = \rho, \quad (5)$$

where  $\mathcal{I}(\cdot)$  is an indicator function which outputs 1 if the input condition is true and 0 otherwise,  $\Delta_{pq}$  denotes a pixel in  $\Delta$ , and  $\rho$  is an user defined parameter controlling the allowable number of pixels which can be perturbed.

### 3.4 Differential Evolution based Optimization

Due to the black-box setting and the complex nature of problem  $\mathcal{Q}$  in (3), standard gradient-based optimization cannot be used to obtain an efficient solution. Instead one may employ EvO techniques in an attempt to find a near-optimal solution after a finite number of generations. An EvO algorithm achieves this by iteratively improving the quality of a population of candidate solutions through exploration (diversifying coarse search in large volume) and exploitation (intensifying detailed search in small volume) of the search space [20]. Among the various EvO techniques tailored for diverse optimization problems, DE is known to be highly effective for real-valued, global optimization problems like  $\mathcal{Q}$  [5]. Due to the large scale and high-dimensional nature of  $\mathcal{Q}$ , we specifically incorporate some modifications to equip DE for the task, resulting in the DEceit algorithm.

$$\Delta'_i \leftarrow \begin{bmatrix} p^{(1)} & q^{(1)} & r_1^{(1)} & \dots & r_c^{(1)} & \dots & p^{(\rho)} & q^{(\rho)} & r_1^{(\rho)} & \dots & r_c^{(\rho)} \end{bmatrix}$$

**Figure 3:** A perturbation  $\Delta_i$  encoded as  $\Delta'_i$  for using in DEceit. The total dimension of the encoding is  $(c + 2) \times \rho$ , which may be considered as  $\rho$  groups of  $(c + 2)$  elements. Given such a group the first two elements  $p^{(i)}$  and  $q^{(i)}$  denote the position respective to width and height of the  $i$ -th pixel to be perturbed, where  $i = 1, 2, \dots, \rho$ . On the other hand, the last  $c$  places  $r_1^{(i)}, r_2^{(i)}, \dots, r_c^{(i)}$  hold the noises for the  $c$  channels. Such an encoding can directly handle the sparsity constraint (5) by implicitly considering the value of  $\rho$  during design.

### 3.4.1 Algorithm Overview:

Before proceeding to a detailed discussion, we first provide a schematic workflow of DEceit in Figure 2 to highlight the key steps involved in the process. Given the problem  $\mathcal{Q}$ , the DEceit algorithm starts by randomly initializing a population  $N = \{\Delta_1, \Delta_2, \dots, \Delta_n\}$  of  $n$  candidate perturbations. However, simply representing a perturbation as a natural tensor of the same size of the original image will not be effective as the different evolutionary operations may end up violating the sparsity constraint (5). Thus, during the DE operations instead of the original perturbation tensor  $\Delta_i$  we consider an encoded vector representation  $\Delta'_i$  having a dimension of  $(c + 2) \times \rho$  as detailed in Figure 3, which by design adheres to (5). Hereafter, we denote an encoded perturbation using a dashed notation of their tensor counterpart. Thereafter, every iteration of DEceit consists of the following four steps: First, a trial solution  $\Gamma'_i$  corresponding to each of the current solutions  $\Delta'_i$  is created as a linear combination of three other candidate solutions using one of the following mutation schemes as explained in the subsequent section discussing mutation switching strategy:

$$\text{DE/rand/1:} \quad \Gamma'_i = \Delta'_{u1} + F(\Delta'_{u2} - \Delta'_{u3}), \text{ or} \quad (6)$$

$$\text{DE/best/1:} \quad \Gamma'_i = \Delta'_b + F(\Delta'_{u2} - \Delta'_{u3}), \quad (7)$$

where  $F$  is the scale-factor,  $\Delta'_b$  is the encoded representation of the best perturbation in  $N$ , and  $\Delta'_{u1}, \Delta'_{u2}, \Delta'_{u3}$  are selected randomly from  $N$  without replacement and differ from the current solution  $\Delta'_i$ . Following mutation,  $\Gamma'_i$  goes through an arithmetic crossover operation as shown in (8) to generate the final offspring solution  $\Theta'_i$  as average of  $\Gamma'_i$  and the corresponding candidate solution  $\Delta'_i$ :

$$\Theta'_i = 0.5\Delta'_i + 0.5\Gamma'_i. \quad (8)$$

The generated offspring vector  $\Theta'_i$  is subsequently corrected (as explained during the discussion on bound correction) to adhere to constraint (4) and decoded to retrieve the perturbation  $\Theta_i$ . Finally in the selection stage,  $\Theta_i$  is compared with the corresponding decoded candidate solution  $\Delta_i$  so as to greedily retain the encoded form of the better of the two in  $N$ :

$$\Delta'_i = \begin{cases} \Theta'_i & \text{if } \mathcal{Q}(\Theta_i) \geq \mathcal{Q}(\Delta_i), \\ \Delta'_i & \text{otherwise.} \end{cases} \quad (9)$$



### 3.4.2 Mutation Switching Strategy:

Only exploratory search will result in delayed or no convergence whereas an only exploitative search might push the population towards a local optimum. Striking a proper balance between these two extremes is critical for high-dimensional search scenarios. The DEceit search mechanism is controlled together by the scale factor  $F$  and the chosen mutation strategy. For every candidate solution in the population, we switch the value of  $F$  between 0.5 and 2 in a uniformly randomized way. When  $F$  attains the larger value, the greater weighting of the difference ( $\Delta'_{u2} - \Delta'_{u3}$ ) helps to the formation of a trial solution which is distant from base solution ( $\Delta'_{u1}$  or  $\Delta'_b$  depending on the chosen mutation strategy). On the other hand, when  $F$  attains the value of 0.5, the trial solution lies close to the current base member ( $\Delta'_{u1}$  or  $\Delta'_b$ ), leading to exploitation of already identified regions of the search space. The choice of  $F$  in a uniform random manner can help stagnant solutions out of local minima.

While the ‘DE/rand/1’ mutation strategy encourages exploration or exploitation based on the chosen  $F$ , ‘DE/best/1’ draws the population close to the current best solution. DEceit chooses either of the two mutation strategies for every candidate solution, in every generation, based on the success history in the last generation. This means that the same mutation strategy as the last generation is retained only if it had resulted in a final offspring superior to the corresponding candidate solution. Thus, the scale factor and mutation strategy together decide the trade-off between the exploratory and exploitative searching capability of DEceit.

### 3.4.3 Bound Corrections:

While the encoding implicitly handles the sparsity constraint (5), the algebraic operations in mutation and crossover may still result in an invalid offspring. Considering the case for the  $i$ -th pixel to be perturbed where  $i = 1, 2, \dots, c$ , a constraint violation may happen in the following three ways, all of which can be easily rectified. First, if any of the location specifiers  $p^{(i)}$  and  $q^{(i)}$  is not an integer, then they can be set to their ceiling values. Second, if any of  $p^{(i)}$  and  $q^{(i)}$  do not respectively lie in the range of  $[1, w]$  and  $[1, h]$ , then they can be reinitialized in their corresponding range. Third, if any of  $r_1^{(i)}, r_2^{(i)}, \dots, r_c^{(i)}$  fails to satisfy the bound constraint (4), then the concerned component can be rectified by reinitializing with a real number between  $-\beta$  and  $\beta$ . We detail the complete method in Algorithm 1.

## 4 Experimental Evaluation

All of our experiments are performed on ImageNet 2012 validation set [23], containing 50000 images spread across 1000 classes. To tackle the issue of diverse

---

**Algorithm 1** DEceit

---

**Input:**  $\mathcal{S}$ : Set of images for UAA/ singleton for IDA.  $\rho$ : Number of allowable pixels for perturbation (if sparsity is not required then set  $\rho = wh$ ).  $t$ : Maximum allowable epochs,  $n$ : Population size.

**Output:** An adversarial perturbation  $\Delta$ .

---

- 1: Randomly initialize  $n$  perturbations  $\Delta_1, \Delta_2, \dots, \Delta_n$ , such that all  $\Delta_i \in \mathbb{R}^{w \times h \times c}$  and follow constraints (4-5). Form a population  $N = \{\Delta'_1, \Delta'_2, \dots, \Delta'_n\}$  by encoding  $\Delta_i$ s for all  $i \in \{1, 2, \dots, n\}$ . Randomly initialize vector  $\mathbf{s} = \{s_i | s_i \in \{0, 1\}, \forall i \in [1, n]\}$ . Calculate the initial fitness as  $\mathbf{e} = \{e_i | e_i = \mathcal{Q}(\Delta_i), \forall i \in [1, n]\}$ .
  - 2: **for**  $t$  epochs **do**
  - 3:   **for**  $i \in [1, n]$  **do**
  - 4:     Select a random scale-factor  $F \in \{0.5, 2\}$ .
  - 5:     If  $s_i = 0$ , then generate mutated solution  $\Gamma'_i$  as per (6). Otherwise, generate  $\Gamma'_i$  as per (7).
  - 6:     Perform crossover to generate perturbation  $\Theta'_i$  by (8).
  - 7:     Perform bound corrections on  $\Theta'_i$  and retrieve  $\Theta_i$ .
  - 8:     Perform selection as per (9). If  $\Delta_i$  is selected over  $\Theta_i$  then set  $s_i = 1 - s_i$ . Otherwise, set  $\Delta'_i = \Theta'_i$  and  $e_i = \mathcal{Q}(\Theta_i)$ .
  - 9:   **end for**
  - 10: **end for**
  - 11: Return the best performing perturbation  $\Delta_b$ .
- 

resolution we have extracted a  $224 \times 224$  center patch from each of the images. We have chosen two state-of-the-art CNN classifiers namely VGG16 [24] and Inception<sup>1</sup> [27, 29].

To quantitatively evaluate the performance of DEceit we have used the conventional FR index, while the visual similarity of the perturbed image with the corresponding original one is measured by Peak Signal to Noise Ratio (PSNR) [11]. To attenuate any bias which may originate from the randomness implicit to DEceit, we report the median result among 11 independent runs in all our experiments. The number of population members of DEceit is set to 50, while the number of generations is set to be 50.

## 4.1 Ablation Study

We start by justifying the motivation behind DEceit through an ablation study detailed in Table 1. We can observe that compared to a benchmark of absolute random perturbations, better UAA can be performed if only the distortions are allowed to be optimized by EvO algorithm such as DE at random pre-determined pixel positions. If we allow both the pixel locations and the distortion to be optimized by EvO algorithms by maximizing  $\mathcal{Q}$ , then an even higher FR can be achieved despite the number of perturbed pixels being greatly reduced. However, compared

---

<sup>1</sup>Depending on the result reported by the contending algorithm Inception may mean either GoogleNet or Inception V3.

to other widely popular EvO algorithms such as GA [1] and CMA-ES [10], DE achieves a better FR validating its applicability to the problem of adversarial attack generation. However, as mentioned earlier, vanilla DE is not tailored to handle a large-scale, high-dimensional optimization problem. Thus replacing it with DEceit further improves in performance as can be seen by contrasting the last two results in Table 1.

Table 1: Ablation study of DEceit on performing UAA.

Method	$\rho$	$\beta$	Fooling Rate (%)	
			VGG16	Inception
Random pixels randomly perturbed	200*	128	35.14	34.22
Random pixels perturbed by DE	200*	128	37.96	36.94
$\mathcal{Q}$ optimized by GA	10	128	38.02	37.03
$\mathcal{Q}$ optimized by CMA-ES	10	128	38.11	37.15
$\mathcal{Q}$ optimized by DE	10	128	39.22	37.86
DEceit (Ours)	10	128	<b>46.79</b>	<b>44.23</b>

\*: To compensate for an unoptimized perturbation we set a higher  $\rho$  at 200.

## 4.2 Universal Adversarial Attacks

We compare DEceit with the state-of-the-art universal non-targeted attack methods namely UAP [15], FFF [17], NAG [18], and GAP [22] in Table 2<sup>2</sup>. We observe from Table 2 that on VGG16 the proposed method outperforms the competitors while being the second best on Inception in terms of both the measures, when all pixels are perturbed (with identical  $\beta$ ). This indicates that DEceit is indeed capable of achieving a competitive performance. Moreover, a qualitative comparison of the generated universal perturbations for UAP, FFF, and DEceit is presented in Figure 4. It is evident from Figure 4 that compared to UAP and FFF the two benchmark white box UAA techniques, the adversarial examples generated by black box method DEceit are minimally distorted from their corresponding original images, even when all pixels are allowed to be perturbed. From Table 2 and Figure 1, we observe that with increasing sparsity, the FR decreases while the PSNR improves. However DEceit provides a perturbation of commendable quality while preserving the visual similarity by only manipulating about 10% of the total pixels.

To further evaluate the robustness of DEceit compared to its contenders, we conduct a transferability [22] study. From Table 3 we observe that all three variants of DEceit achieve better transferability than the other methods<sup>3</sup> on both classifiers, demonstrating the higher robustness of the proposed method. Interestingly, the perturbation generated by NAG which performs well on Inception (as observed in Table 2) fails on VGG16, indicating its lower robustness compared to DEceit.

<sup>2</sup>Results are quoted from the original articles.

<sup>3</sup>For GAP no transferability to Inception is available.

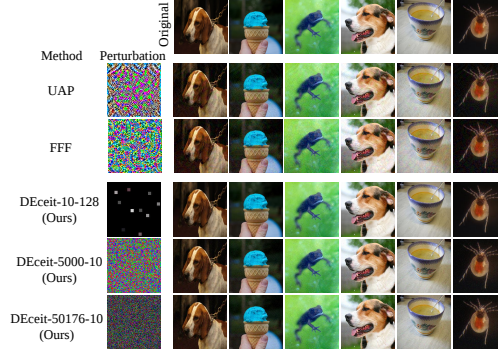


Figure 4: We take six images from ImageNet 2012 validation set and apply the perturbation obtained from UAP, FFF (for UAP and FFF pre-trained perturbations are obtained from the original articles), and DEceit (the different variants are named as DEceit- $\rho$ - $\beta$ ). In all cases, the perturbed image is misclassified by the pre-trained VGG16. We can see that compared to the white-box methods, DEceit can generate a successful adversarial example with minimal distortion. The effect of perturbation (the values of the perturbed pixels are propagated to their neighbors for the ease of visualization) is almost imperceptible when  $\rho = 10$ . Even though with  $\rho = 50176$ , DEceit generates perturbed images where the distortion is somewhat apparent, the visual quality is still better compared to UAP and FFF.

Table 2: Comparison of DEceit with non-targeted UAA methods.

Method	$\rho$	$\beta$	Fooling Rate (%)			PSNR (dB)		
			VGG16	Inception V3	GoogleNet	VGG16	Inception V3	GoogleNet
UAP	50176	10	78.37	NA	77.74	29.25	NA	28.45
FFF	50176	10	47.25	NA	56.59	27.12	NA	24.56
NAG	50176	10	77.57	<b>90.37</b>	NA	NA	NA	NA
GAP	50176	10	83.70	82.70	NA	NA	NA	NA
DEceit (Ours)	10	128	46.79	44.23	44.44	<b>65.12</b>	<b>65.01</b>	<b>68.99</b>
	100	30	56.22	52.86	54.55	56.76	57.01	58.69
	1000	20	62.05	53.11	57.69	48.25	48.22	49.58
	5000	10	65.66	59.55	61.56	44.16	45.01	46.89
	10000	10	68.95	63.25	66.89	38.96	37.57	39.44
	50176	10	<b>83.96</b>	83.03	<b>84.96</b>	33.14	32.99	33.25

NA: The pre-trained perturbations are not available for computing Fooling Rate & PSNR.

Moreover, the transferability of DEceit only slightly changes with the choices of  $\rho$ , suggesting that the proposed method is mostly resilient to the extent of sparsity. Such improved robustness of DEceit possibly arises due to its black-box setting and the efficient search capability.

### 4.3 Image-Dependent Attacks

While we primarily developed DEceit for UAAs, it can directly be applied for IDA by feeding  $\mathcal{S}$  as a singleton set containing only the image to be perturbed. Following convention we evaluate the efficacy of DEceit for IDA by comparing its performance on a subset of ImageNet 2012 validation set (containing 2000 correctly classified images) with the state-of-the-art such as PBBA [14], GAP [22], LogBarrier [6], SIMBA [19], GenAttack [1], SparseFool [13], and OPA [26] in

Table 3: Transferability of DEceit compared to UAA methods.

Method	$\rho$	$\beta$	Transferability (%)	
			VGG16 <sup>4</sup>	Inception <sup>5</sup>
UAP	50176	10	89.64	92.71
FFF	50176	10	74.52	71.66
NAG	50176	10	86.86	62.41
DEceit (Ours)	10	128	<b>99.98</b>	<b>96.79</b>
	5000	10	99.84	95.83
	50176	10	99.14	95.21

<sup>4</sup>Transferability from VGG16 to Inception.<sup>5</sup>Transferability from Inception to VGG16.

Table 4: Comparison of DEceit with non-targeted IDA methods.

Method	$\rho$	$\beta$	No. of Images	Attacked Network	Avg. Query	Fooling Rate (%)
PBBA	50176	0.05	50000	Inc. V3	722	98.5
DEceit (Ours)	50176	0.05	2000	Inc. V3	<b>535</b>	<u>99.2</u>
GAP	50176	10	50000	Inc. V3	NA	98.3
DEceit (Ours)	50176	10	2000	Inc. V3	NA	<u>100</u>
LogBarrier	50176	8	500	ResNet 50	NA	95.2
DEceit (Ours)	50176	8	2000	ResNet 50	NA	<b>99.1</b>
SIMBA	50176	3	1000	Inc. V3	1284	97.8
DEceit (Ours)	50176	3	2000	Inc. V3	<b>650</b>	<b>98.1</b>
GenAttack	50176	0.05	2000	Inc. V3	11081	78.4
DEceit (Ours)	50176	0.05	2000	Inc. V3	<b>535</b>	<b>99.2</b>
SparseFool	7024 <sup>6</sup>	255	2000	Inc. V3	NA	<b>100</b>
DEceit (Ours)	7024	255	2000	Inc. V3	NA	<b>100</b>
OPA	1	128	2000	Inc. V3	NA	37.25
DEceit (Ours)	1	128	2000	Inc. V3	NA	<b>46.12</b>

<sup>6</sup>Average number of perturbed pixels.

Table 4. SparseFool (with default parameter setting) and DEceit are evaluated on the same set of images, while the results of the other contenders are quoted from the original papers (DEceit is run with identical  $\rho$  and  $\beta$ ). However, the comparative study may only be considered as indicative as the contending algorithms may have been run on different random sets of images. We can observe from Table 4 that compared to PBBA and GAP our method achieves a competitive FR on a lesser number of images. Moreover, DEceit outperforms (even on higher number of images) LogBarrier, SIMBA, GenAttack, and OPA, using a lesser number of average queries, supporting its efficiency in performing IDA. Further, DEceit performs comparable to SparseFool, while incurring a higher computational cost. However, unlike SparseFool, the proposed DEceit is a black-box technique which can be directly extended to UAA and thus can serve as an attractive alternative.

## 5 Conclusion

In this article, we introduced DEceit, a black-box pixel-restricted universal (non-targeted) adversarial perturbation technique. We expressed the task of finding a universal perturbation as a constrained optimization problem. For effectively solving this real-valued high-dimensional optimization problem, we devised DEceit by modifying the DE algorithm through the incorporation of a novel mix of the mutation switching strategy along with a uniform random scale-factor switching scheme. We also introduced an encoding scheme which can implicitly impose the sparsity constraint. Finally, we empirically validated the capability of DEceit to perform effective, imperceptible, and robust adversarial attacks.

A direct extension of our work may focus on the two contradictory objectives of maximizing the effectiveness of a perturbation while minimizing the visual distortions, which can be expressed in the form of a high-dimensional multi-objective optimization problem, solvable by a tailored DE variant. One may also consider using DEceit for searching a perturbation in a transformed space instead of the native image space, following [9].

## References

- [1] M. Alzantot, Y. Sharma, S. Chakraborty, H. Zhang, C.-J. Hsieh, and M. B. Srivastava. GenAttack: practical black-box attacks with gradient-free optimization. In *ACM GECCO*, page 1111–1119, 2019.
- [2] N. Carlini and D. Wagner. Towards evaluating the robustness of neural networks. In *IEEE S&P*, pages 39–57, 2017.
- [3] F. Croce and M. Hein. Sparse and imperceptible adversarial attacks. In *IEEE ICCV*, 2019.
- [4] H. Dang, Y. Huang, and E.-C. Chang. Evading classifiers by morphing in the dark. In *ACM CCS*, pages 119–133, 2017.
- [5] S. Das, S. S. Mullick, and P. N. Suganthan. Recent advances in differential evolution—an updated survey. *Swarm and Evolutionary Computation*, 27:1–30, 2016.
- [6] C. Finlay, A.-A. Pooladian, and A. Oberman. The logbarrier adversarial attack: Making effective use of decision boundary information. In *IEEE ICCV*, 2019.

- [7] A. Ghosh, S. Das, S. S. Mullick, R. Mallipeddi, and A. K. Das. A switched parameter differential evolution with optional blending crossover for scalable numerical optimization. *App. Soft Comp.*, 57:329–352, 2017.
- [8] I. Goodfellow, J. Shlens, and C. Szegedy. Explaining and harnessing adversarial examples. *arXiv preprint arXiv:1412.6572*, 2014.
- [9] C. Guo, J. Gardner, Y. You, A. G. Wilson, and K. Weinberger. Simple black-box adversarial attacks. In *ICML*, pages 2484–2493, 2019.
- [10] N. Hansen. The cma evolution strategy: a comparing review. In *Towards a new evolutionary computation*, pages 75–102. Springer, 2006.
- [11] Alain Hore and Djemel Ziou. Image quality metrics: Psnr vs. ssim. In *IEEE ICPR*, pages 2366–2369, 2010.
- [12] S. Jetley, N. Lord, and P. Torr. With friends like these, who needs adversaries? In *NIPS*, pages 10749–10759, 2018.
- [13] A. Modas, S.-M. Moosavi-Dezfooli, and P. Frossard. Sparsefool: A few pixels make a big difference. In *IEEE CVPR*, 2019.
- [14] S. Moon, G. An, and H. O. Song. Parsimonious black-box adversarial attacks via efficient combinatorial optimization. In *ICML*, pages 4636–4645, 2019.
- [15] S.-M. Moosavi-Dezfooli, A. Fawzi, O. Fawzi, and P. Frossard. Universal adversarial perturbations. In *IEEE CVPR*, pages 1765–1773, 2017.
- [16] S.-M. Moosavi-Dezfooli, A. Fawzi, and P. Frossard. Deepfool: a simple and accurate method to fool deep neural networks. In *IEEE CVPR*, pages 2574–2582, 2016.
- [17] K. R. Mopuri, U. Garg, and R. V. Babu. Fast feature fool: A data independent approach to universal adversarial perturbations. In *BMVC*, 2017.
- [18] K. R. Mopuri, U. Ojha, U. Garg, and R. V. Babu. NAG: Network for adversary generation. In *IEEE CVPR*, June 2018.
- [19] N. Narodytska and S. Kasiviswanathan. Simple black-box adversarial attacks on deep neural networks. In *IEEE CVPR Workshops*, pages 6–14, 2017.
- [20] K. R. Opara and J. Arabas. Differential evolution: A survey of theoretical analyses. *Swarm and Evolutionary Computation*, 44:546 – 558, 2019.

- [21] N. Papernot, P. McDaniel, I. Goodfellow, S. Jha, Z. B. Celik, and A. Swami. Practical black-box attacks against machine learning. In *ASIA-CCS*, pages 506–519, 2017.
- [22] O. Poursaeed, I. Katsman, B. Gao, and S. Belongie. Generative adversarial perturbations. In *IEEE CVPR*, pages 4422–4431, 2018.
- [23] O. Russakovsky, J. Deng, H. Su, J. Krause, S. Satheesh, S. Ma, Z. Huang, A. Karpathy, A. Khosla, M. Bernstein, A. C. Berg, and F.-F. Li. ImageNet Large Scale Visual Recognition Challenge. *IJCV*, 115(3):211–252, 2015.
- [24] K. Simonyan and A. Zisserman. Very deep convolutional networks for large-scale image recognition. *arXiv preprint arXiv:1409.1556*, 2014.
- [25] R. Storn and K. Price. Differential evolution—a simple and efficient heuristic for global optimization over continuous spaces. *Journal of global optimization*, 11(4):341–359, 1997.
- [26] J. Su, D. V. Vargas, and K. Sakurai. One pixel attack for fooling deep neural networks. *IEEE Tran. on Evo. Comp.*, 2019.
- [27] C. Szegedy, V. Vanhoucke, S. Ioffe, J. Shlens, and Z. Wojna. Rethinking the inception architecture for computer vision. In *IEEE CVPR*, pages 2818–2826, 2016.
- [28] C. Szegedy, W. Zaremba, I. Sutskever, J. Bruna, D. Erhan, I. Goodfellow, and R. Fergus. Intriguing properties of neural networks. *arXiv preprint arXiv:1312.6199*, 2013.
- [29] W. Szegedy, C. and Liu, Y. Jia, P. Sermanet, S. Reed, D. Anguelov, D. Erhan, V. Vanhoucke, and A. Rabinovich. Going deeper with convolutions. In *IEEE CVPR*, pages 1–9, 2015.
- [30] P. Zhao, S. Liu, P.-Y. Chen, N. Hoang, K. Xu, B. Kailkhura, and X. Lin. On the design of black-box adversarial examples by leveraging gradient-free optimization and operator splitting method. In *IEEE ICCV*, 2019.